Transient Multiphysics Simulations on Blue Waters and Their Applications in Improvement of Steel Continuous Casting

Illinois General Project:
Fluid-Flow and Stress Analysis of Steel Continuous Casting

Seong-Mook Cho[1] (Co-PI and Presenter) and Brian G. Thomas[1,2] (PI)

1. Department of Mechanical Science and Engineering, University of Illinois at Urbana-Champaign
2. Department of Mechanical Engineering, Colorado School of Mines

Acknowledgements

- Blue Waters / National Center for Supercomputing Applications (NCSA) at UIUC
- Co-PIs at U-Illinois: Kai Jin (previous Ph.D. Student), S.P. Vanka (Emeritus Professor of Mechanical Engineering), Hyunjin Yang (Ph.D. Student), Matthew Zappulla (previous M.S. Student), Xiaolu Yan (M.S. Student)
- Co-PIs at NCSA: Ahmed Taha (Technical Program Manager), Seid Koric (Adjunct Associate Professor)
- ANSYS. Inc. for Fluent-HPC License Allocation
- Continuous Casting Consortium at UIUC and Continuous Casting Center at CSM Members(ABB, AK Steel, ArcelorMittal, Baosteel, JFE Steel Corp., Magnesita Refractories, Nippon Steel and Sumitomo Metal Corp., Nucor Steel, Postech/Posco, SSAB, ANSYS/Fluent)
- National Science Foundation (Grant Nos.11-30882 and 15-63553)

Recent Publications Acknowledging Blue Waters (2016-2017)

[1] CCC Annual Meeting, Colorado School of Mines, August, 2016

[2] CCC Annual Meeting, Colorado School of Mines, August, 2017, pending

[3] B.G. Thomas, S-M. Cho, K. Jin, P. Vanka, H. Yang, M. Zappulla, X. Yan, A. Taha, and S. Koric: "Transient Two-Phase Flow and Electromagnetic Field Effect in Steel Continuous Casting", Blue Waters Annual Report 2016, ed. B. Jewett, University of Illinois, Urbana, IL, 2016, pp. 101-102.

[4] S-M. Cho, B G. Thomas, and S-H. Kim: "Transient Two-Phase Flow in Slide-Gate Nozzle and Mold of Continuous Steel Slab Casting with and without Double-Ruler Electro-Magnetic Braking", Metallurgical and Materials Transactions B, Vol. 47B (2016), pp. 3080-3098, DOI:10.1007/s11663-016-0752-4

[5] K. Jin, S. P. Vanka, B. G. Thomas: "Large Eddy Simulation of the Effects of EMBr and SEN Submerged Depth on Turbulent Flow in the Mold Region of a Steel Caster", Metallurgical and Materials Transactions B, Vol. 48B (2016), pp. 162-178, DOI:10.1007/s11663-016-0801-z

[6] K. Jin, Surya P. Vanka, Brian G. Thomas, and Xiaoming Ruan: "Large Eddy Simulations of the Effects of Double-Ruler Electromagnetic Braking and Nozzle Submergence Depth on Molten Steel Flow in a Commercial Continuous Casting Mold", Proc. TMS Annual Meeting 2016, Nashville, TN, 2016

[7] K. Jin, P. Kumar , S. P. Vanka and B.G. Thomas: "Rise of an argon bubble in liquid steel in the presence of a transverse magnetic field". Physics of Fluids, Vol. 28 (2016), 093301-1-27. DOI: 10.1063/1.4961561

[8] K. Jin, B.G. Thomas, and X. Ruan: "Modeling and Measurements of Multiphase Flow and Bubble Entrapment in Steel Continuous Casting", Metallurgical and Materials Transactions B, Vol. 47B (2016), pp. 548-565, DOI: 10.1007/s11663-015-0525-5.

[9] K. Jin, S. P. Vanka, and B.G. Thomas: "Large Eddy Simulations of Argon Bubble Transport and Capture in Mold Region of a Continuous Steel Caster", Proc. TFEC2017, Las Vegas, NV, 2017

[10] Matthew L. S. Zappulla, Brian G. Thomas: "Thermal-Mechanical Model of Depression Formation in Steel Continuous Casting", Proc. TMS2017, San Diego, CA, 2017

[11] K. Jin, S. P. Vanka, and B.G. Thomas: "Large Eddy Simulations of Electromagnetic Braking Effects on Argon Bubble Transport and Capture in a Steel Continuous Casting Mold", Metallurgical and Materials Transactions B, under review

[12] S-M. Cho, B G. Thomas, and S-H. Kim, "Effect of Nozzle Port Angle on Transient Flow Variations during Continuous Steel-Slab Caster", in preparation

Introduction I: Continuous Casting of Steel

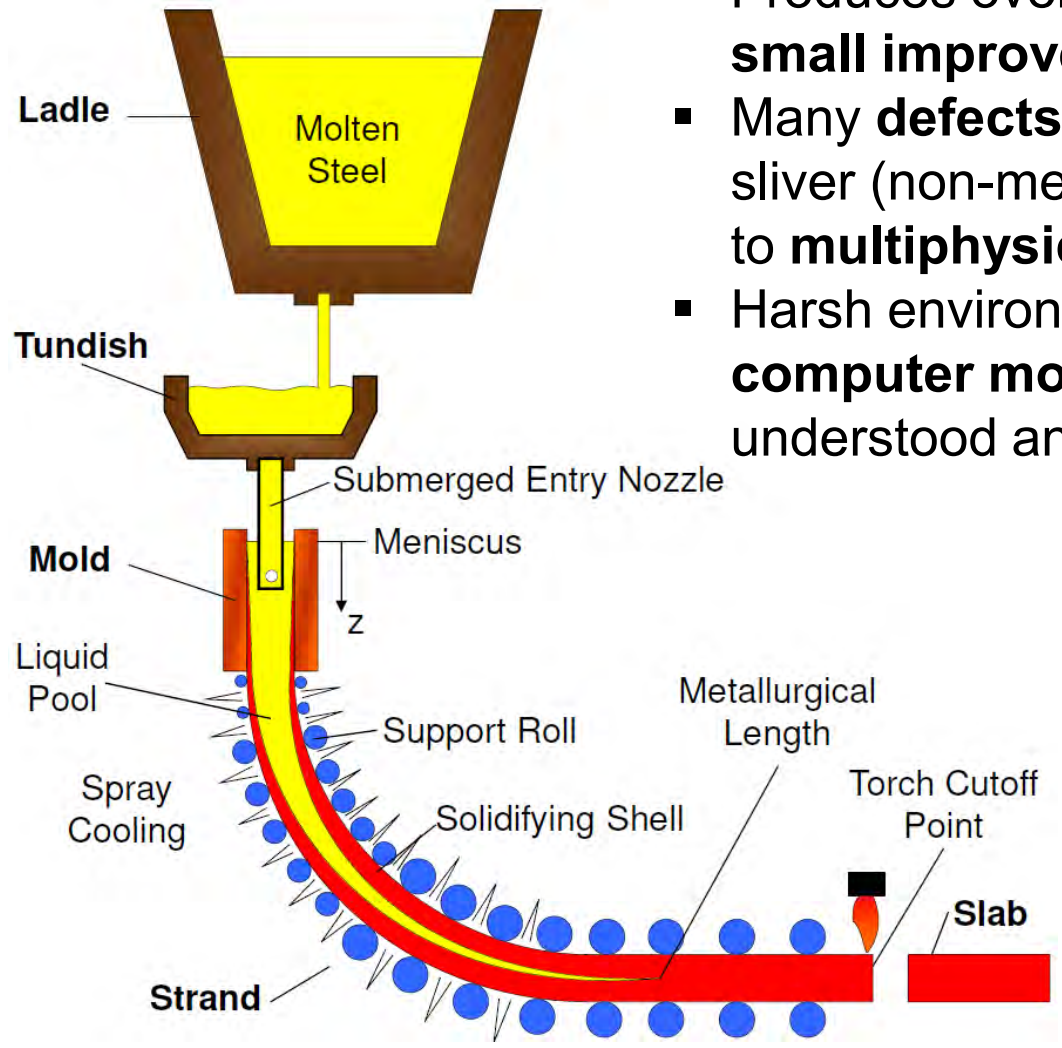

<Schematic of steel continuous casting>

- Produces over **95% of steel** in the world[*], so **small improvements** have **large impact**
- Many **defects** (blister (gas bubble defect) and sliver (non-metallic inclusion defect), etc) related to **multiphysics phenomena** in mold
- Harsh environment makes experiments difficult; **computer models** allow process to be understood and improved

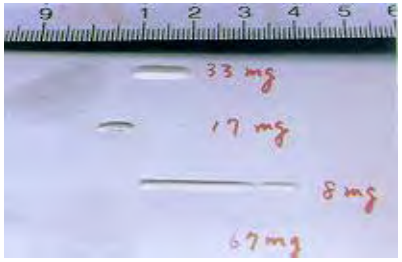

Blister (coil)

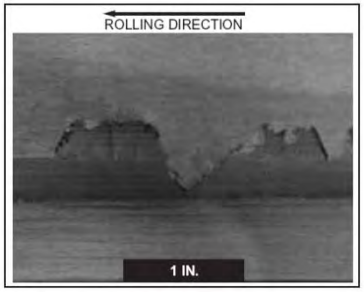

Sliver (coil)

<Defects in final products>

*Steel Statistical Yearbook 2014. (World Steel Association, Brussels, Belgium, 2014)

Introduction II: Complex Phenomena in CC

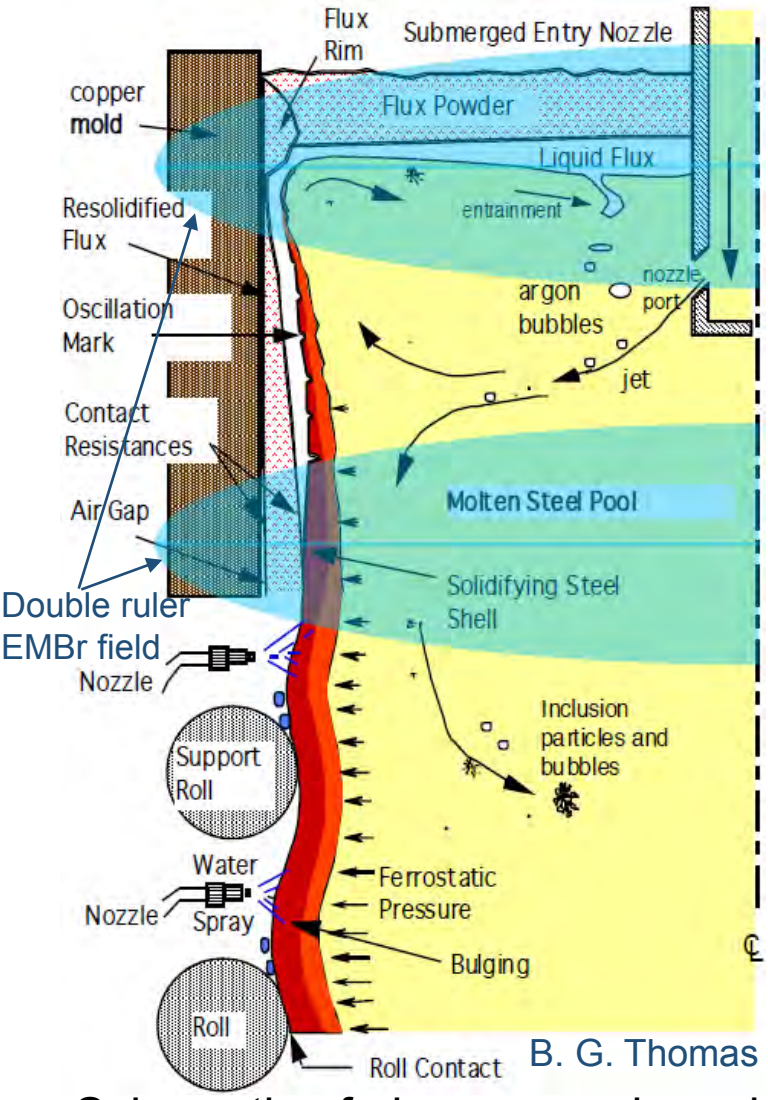

<Schematic of phenomena in mold>

- Turbulent multiphase flow
- Heat transfer & solidification
- Steel/slag interface & surface tension
- Nucleation, collision, growth of steel crystals, bubbles & inclusions
- Transport & removal of particles
- Multiphase thermodynamics
- Mass transfer & segregation
- Deformation & stress
- Microstructure evolution
- Precipitate particles
- Embrittlement & cracks
- Multiple time & size scales
- MagnetoHydroDynamics (MHD)

Introduction III: Multiphysics Phenomena related to Defect Formation in CC

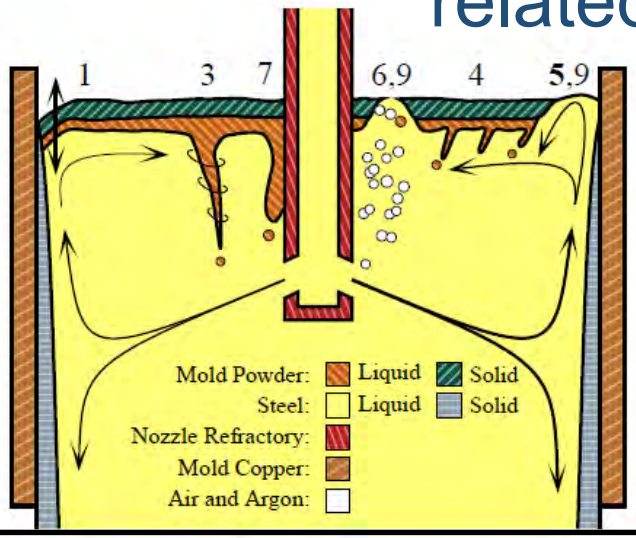

1. Surface fluctuation
2. Meniscus freezing, hook formation
3. Vortex Formation
4. Shear layer instability
5. Upward flow
6. Argon bubble interactions/slag foaming
7. Slag crawling
8. Surface wave instability
9. Surface balding

< Slag entrainment mechanisms[2-4] >

- **Instability at liquid mold flux/molten steel interface**, can **entrain liquid mold flux** into molten steel pool, and produce **capture into steel shell**, resulting in surface or internal defects.
- **Argon bubbles** make **mold flow more complex** and may be **entrapped with non-metallic inclusions by solidifying steel shell**, which can be defects.
- **Meniscus freezing** and **hook formation**, affected by **fluid flow with superheat transportation**, govern steel **solidification** and produce other defects.

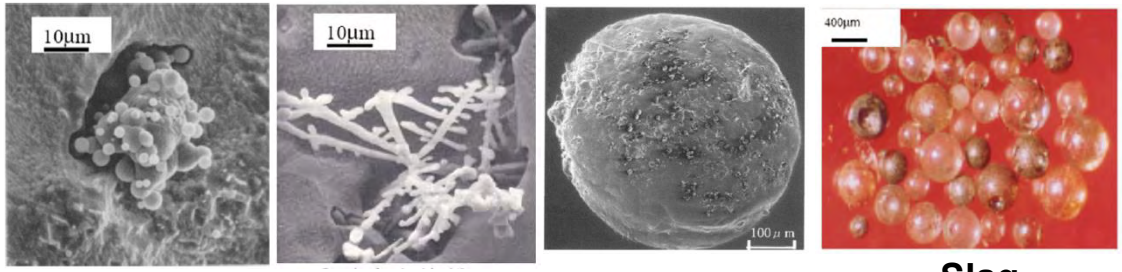

Alumina cluster | **Alumina dendrite** | **Bubble with inclusions** | **Slag inclusions**

<Bubbles and Inclusions entrapped by steel shell[1]>

1. B.G. Thomas, Q. Yuan, S. Mahmood, R. Lui, and R. Chaudhary: MMTB, Vol. 45 , No. 1, P. 22-35 , 2013
2. L. C. Hibbeler, R. Liu, and B. G. Thomas: Proceedings of the 7th European Continuous Casting Conference, Steel Institute VDEh, 2011
3. L. C. Hibbeler and B. G. Thomas: Iron and Steel Technology, Vol. 8, No. 10, P. 121-136, 2013
4. K. E. Swartz, L. C. Hibbeler, B. P. Joyce, and B. G. Thomas: Proceedings of AISTech, AIST, 2014

Computational Models on Blue Waters

- **Why computational model**: limitation of experiments on quantifying and understanding complex multiphysics phenomena related to defect formation in CC, and improving CC process
- **Why Blue Waters**
  - High-resolution (< 1mm length scale) prediction of multiphysics phenomena in huge domain (eg. 0.2 m X 1.9 m X 4.6 m)
  - Speed-up breakthrough (over ~3357X) on computing
- **Applied models: ANSYS FLUENT (commercial CFD code)** and **CUFLOW (in-house multi-GPU based code)**
  - Turbulence models: Large Eddy Simulation (LES), Reynolds-Averaged Navier-Stokes (RANS) model (standard k-ε)
  - Second-phase models: Volume Of Fluid (VOF), Lagrangian Discrete Phase Model (DPM)
  - MagnetoHydroDynamics (MHD) model
  - Heat transfer model
  - Particle capture model (based on local force balances on particles at solidification front)

CUFLOW Configuration

- Two versions of CUFLOW, CPU and GPU versions
  - CPU version, run on multi-CPU PC: data compunication through MPI
  - GPU version, run on multi-GPU PC and multi-CPU&GPU pair supercomputer (eg. Blue Waters)

	PC - 4GPU Workstation	Blue Waters Supercomputer
#of Nodes	1	4224
Node CPU	Xeon E5-2650v2 Ivy Bridge, 2.60 GHz, 8 cores	AMD 6276, 2.3 GHz, 16 cores
GPU/Node	4 × Nvidia Tesla C2075, 4 × **5 GB**, 575 MHz	1 × Nvidia Tesla K20x, 1 × **6 GB**, 732 MHz

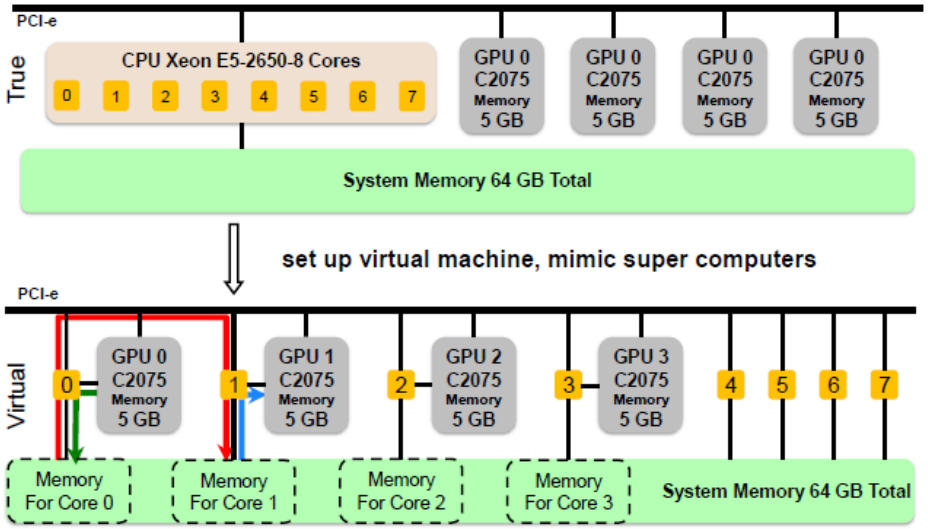

<Configuration of 4 GPU workstation>

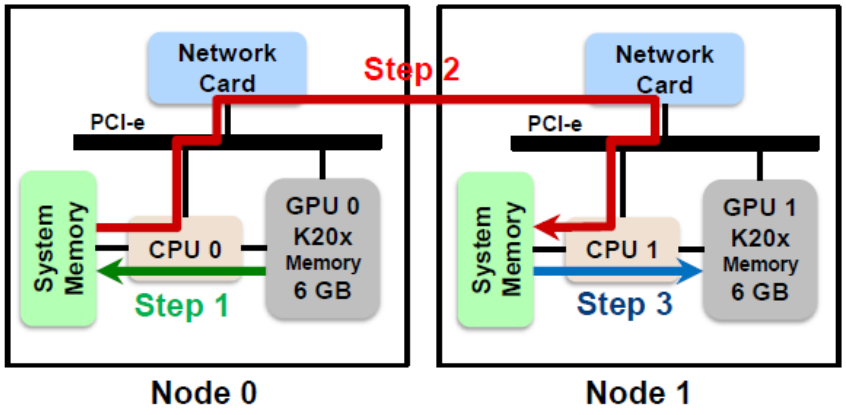

Three Steps: cudaMemcpy(…), MPI_Send(…) and MPI_Recv(…), cudaMemcpy(…)

<Configuration of BW nodes showing 2 nodes>

CUFLOW on Blue Waters

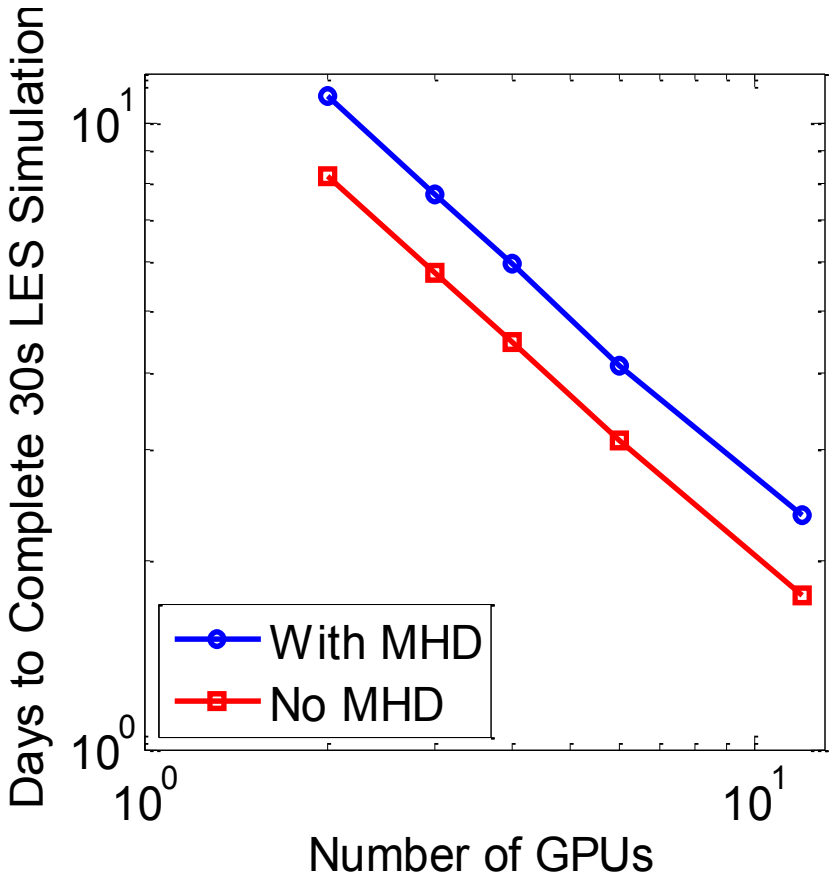

<Estimated time for 30s LES simulation of caster with 14.1 million cells[5]>

- The in-house multi-GPU code CUFLOW has been developed and tested on Blue Waters XK node, which has Nvidia K20x GPU as co-processors, and good speed up has been obtained.
- Less than 2 days are required for a 30s-LES simulation of flow in a caster domain with 14.1 million cells (based on 100 time step test run with average time step size Δt=0.0005s)

ANSYS FLUENT on Blue Waters

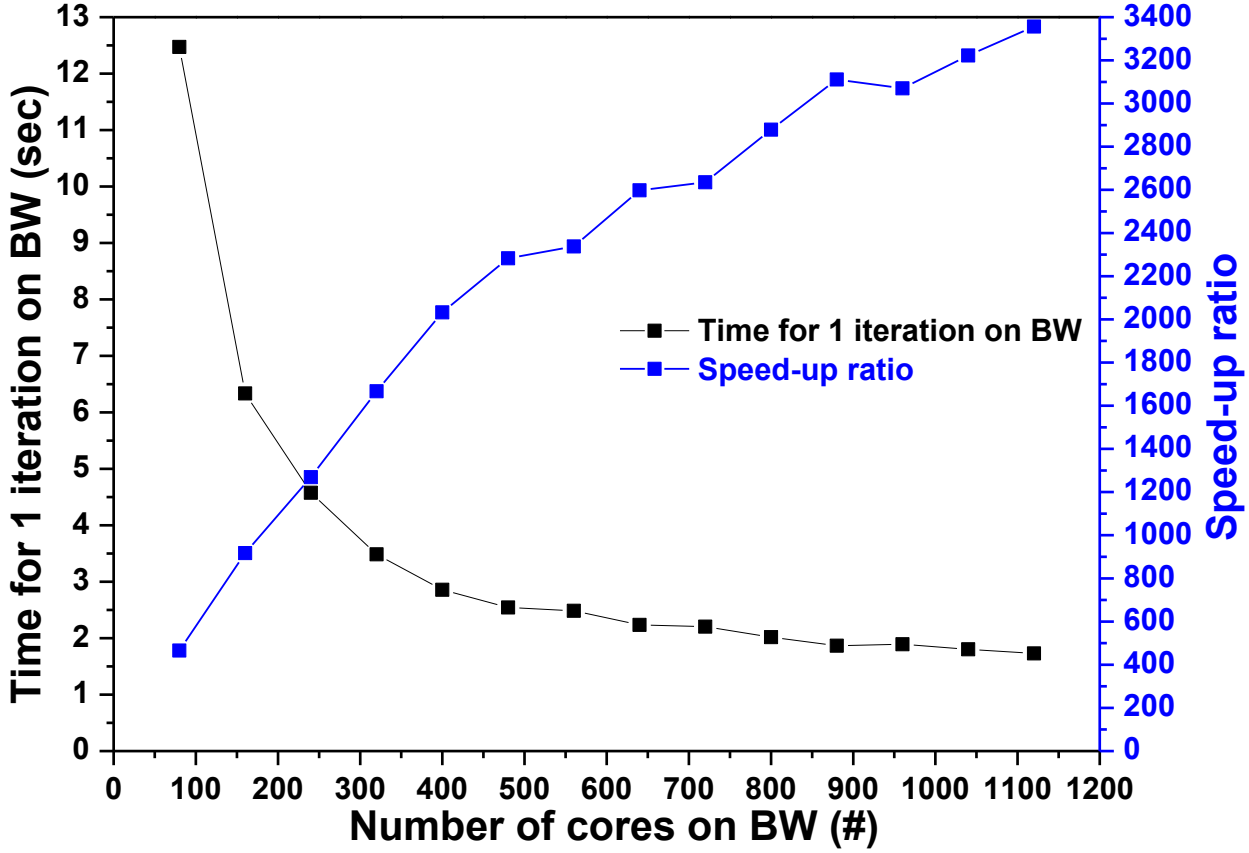

- Lab Computer (LC) calculation: Dell T7600 (Intel ® Xeon ® CPU E5-2603 @ 1.80GHz, RAM 40.0 GB, using 6 cores

- **Speed-up ratio =** Computing time for 1 iteration on **LC /** Computing time for 1 iteration on **BW**

Speed-up test was performed for **LES coupled with VOF** in domain of **~22 million hexahedral cells**

- With **1120 cores (70XE nodes),** the simulation on BW runs **~ 3357 times faster than on our LC**: one iteration on BW using 1120 cores (70 XE nodes) requires **~1.7 seconds** of wall clock time. one the other hand, on the LC, the same simulation requires **~ 5808 seconds** of wall-clock time for 1 iteration.
- For this case, Fluent-14.5 HPC on BW shows **speed-up breakthrough** with 1120 cores (70 XE nodes); **getting much more efficiency for much finer mesh domain**

Research Scope with Blue Waters

- **Objectives:**
  - Get insights into **multiphysics phenomena** and **defect formation**
  - Suggest **optimum CC-process conditions** to improve final steel-product quality
- **Topics:**
  - Effect of **nozzle port angle** on transient mold flow and **liquid slag/molten steel interfacial motion**[1,12]: **LES-VOF** model
  - Effect of **SEN depth** on mold flow[1,5,6]: **LES**
  - **Argon bubble transport** and **capture** in mold with **Electro-Magnetic Braking (EMBr)**[1,3-9,11]: **LES-DPM-Particle capture** model
  - **Transient mold flow** and **superheat transfer** on solidifying steel shell[1,2]: **LES-VOF-Heat transfer** model

CC Domain and Mesh

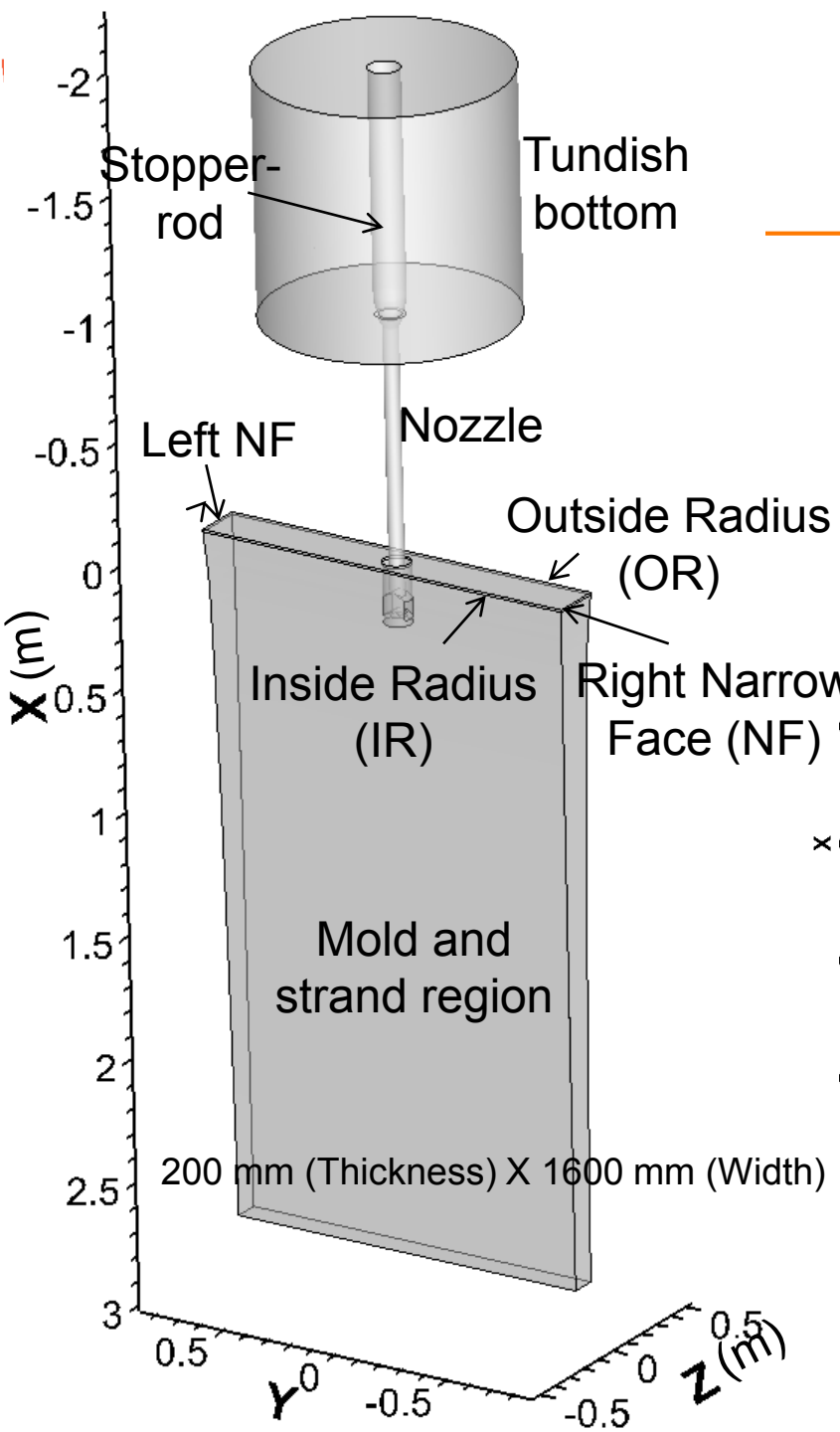

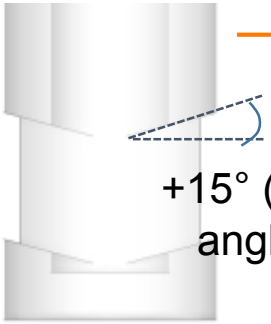

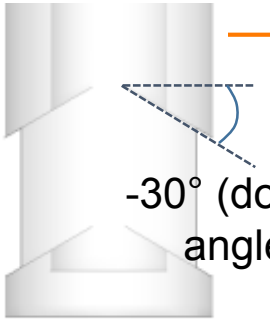

Nozzle port

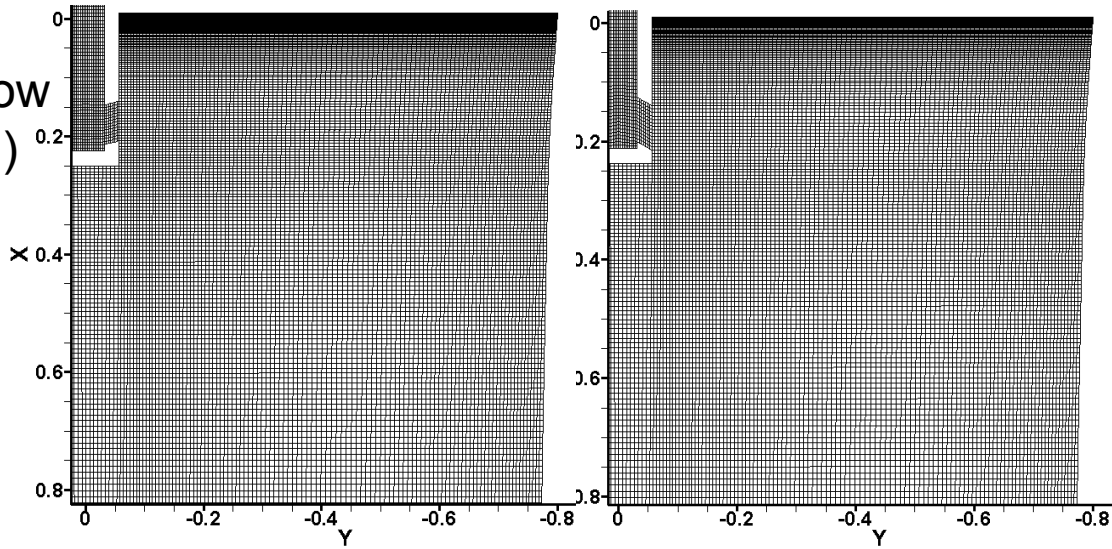

Full domain:~ 4.1 million hexahedral cells

Case 1. +15° (up) angle Case 2. -30° (down) angle

Effect of Nozzle Port Angle: Mold Flow Pattern and Slag Entrainment

- LES coupled with VOF model for molten steel-liquid mold flux flow

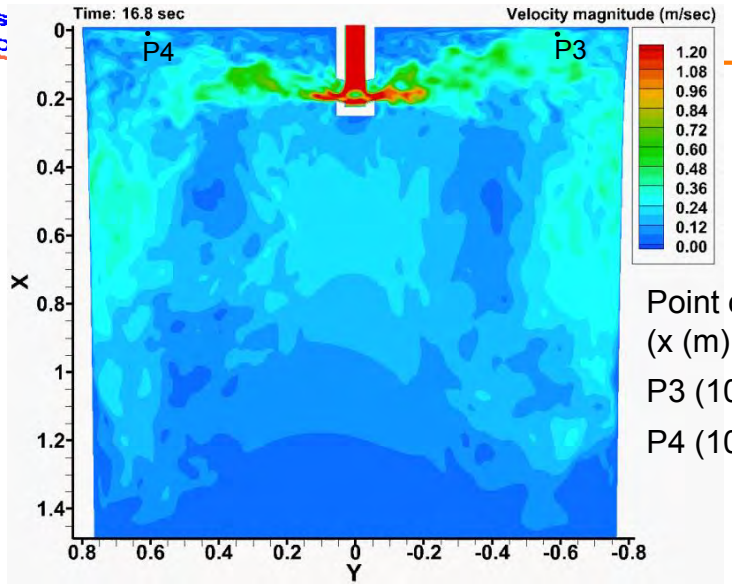

Point coordinate
(x (m), y (m))

P3 (10, -600)

P4 (10, 600)

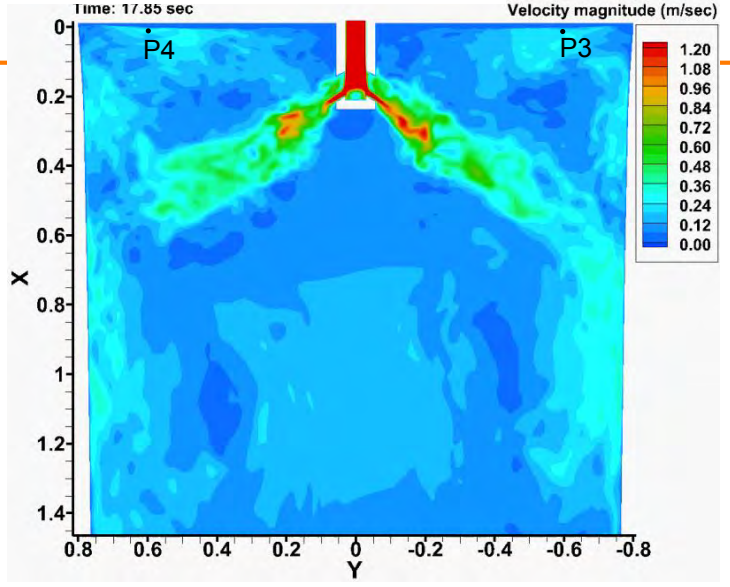

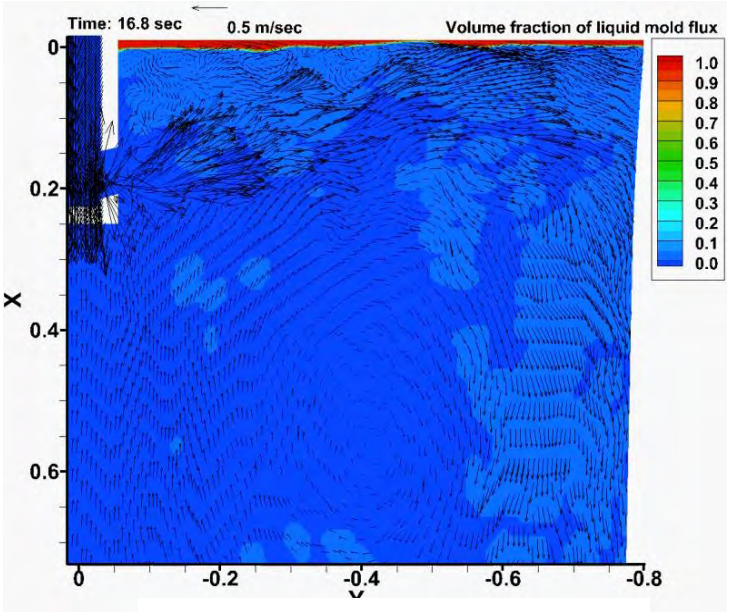

Case 1. +15° (up) angle

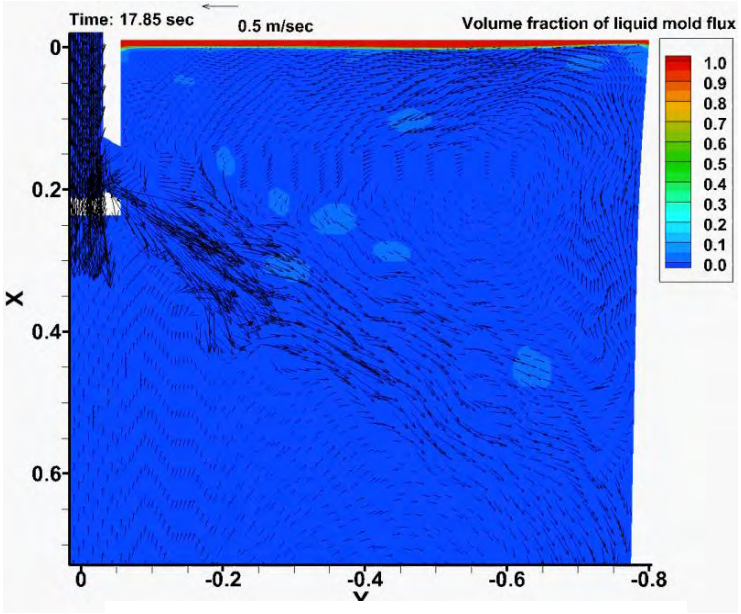

Case 2. -30° (down) angle

Effect of Nozzle Port Angle: Surface Velocity Instability (Model Validation)

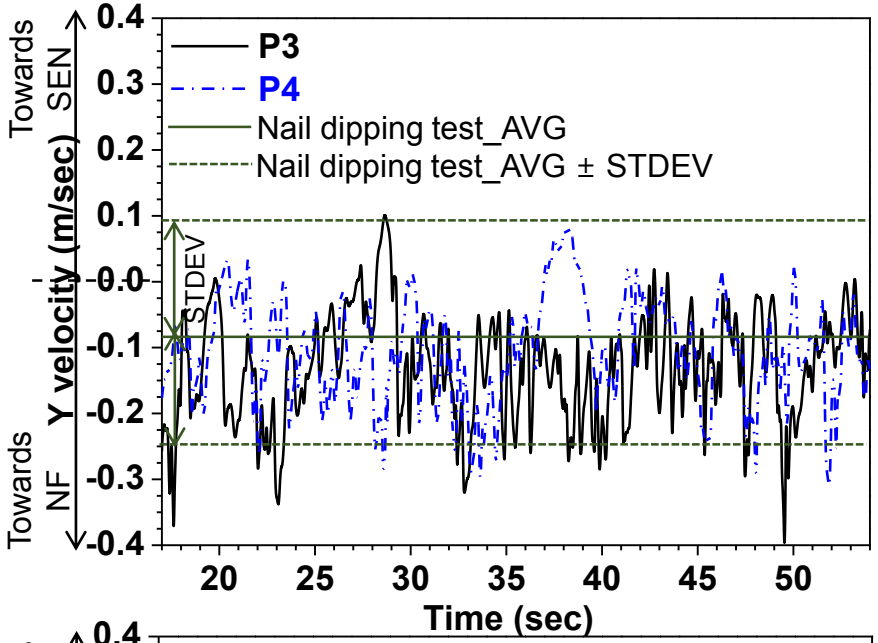

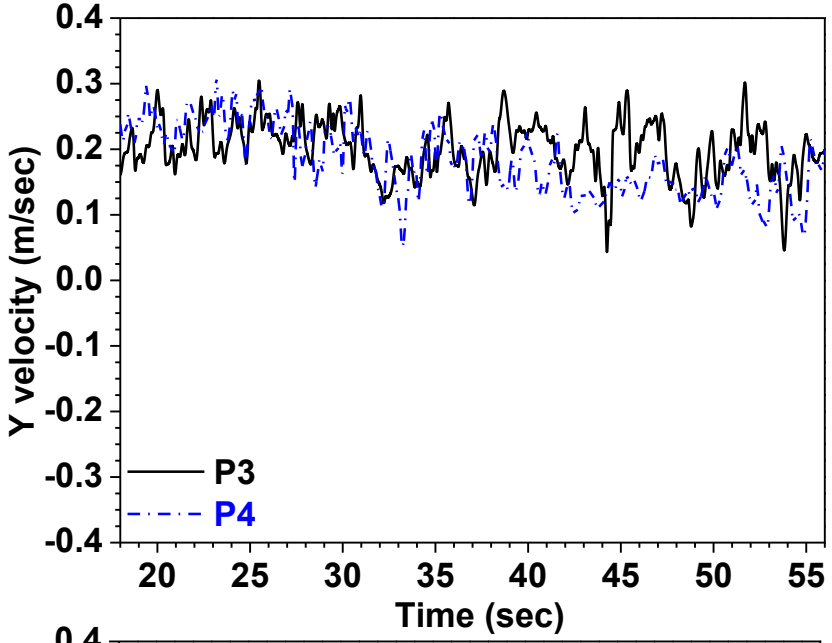

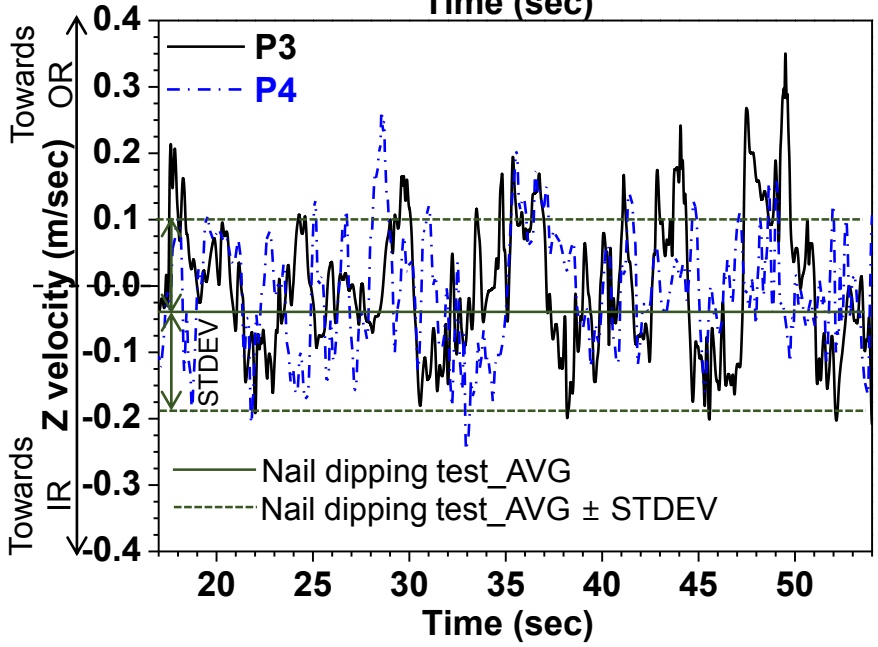

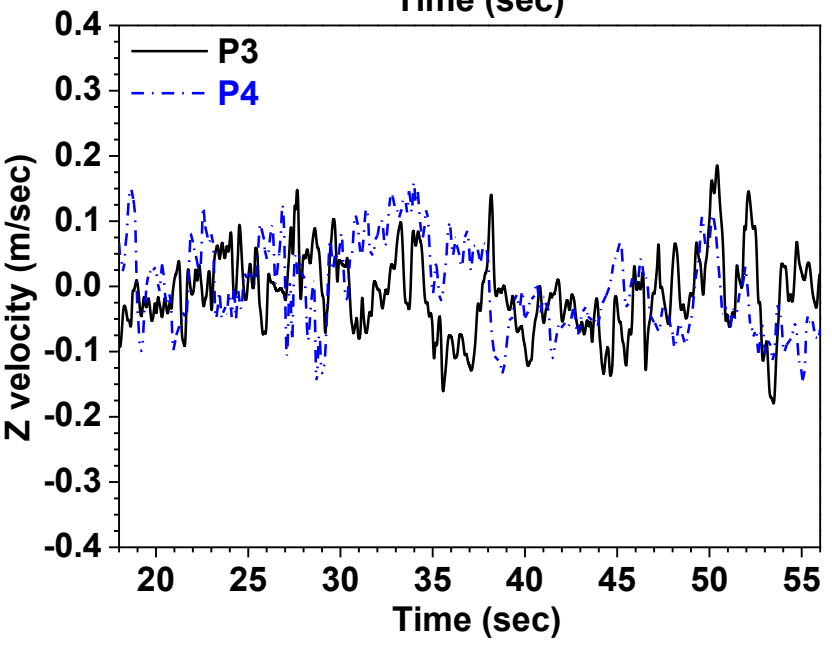

Case 1. +15° (up) angle

Case 2. -30° (down) angle

Effect of Nozzle Port Angle: Surface Level Instability and Defect Formation

More variations at liquid mold flux/molten steel interface in mold with upward angled nozzle port

⇩

<Slag defects on final plates>

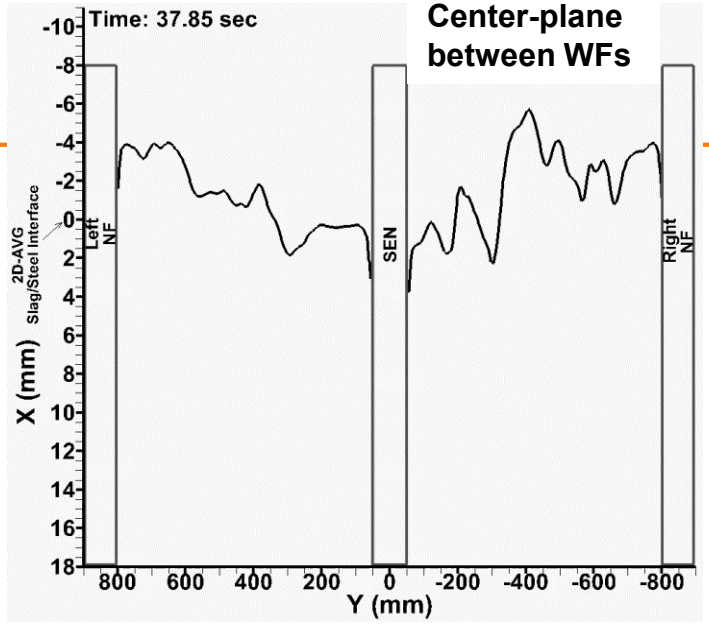

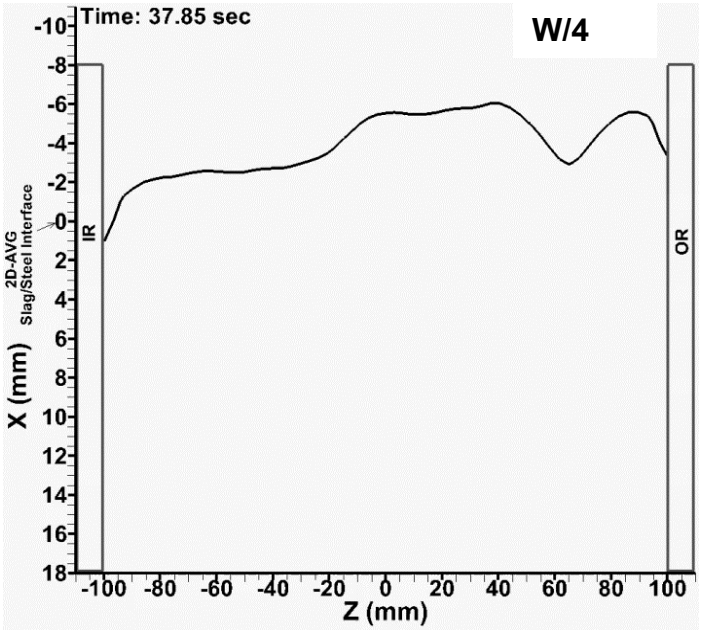

Case 1. +15° (up) angle

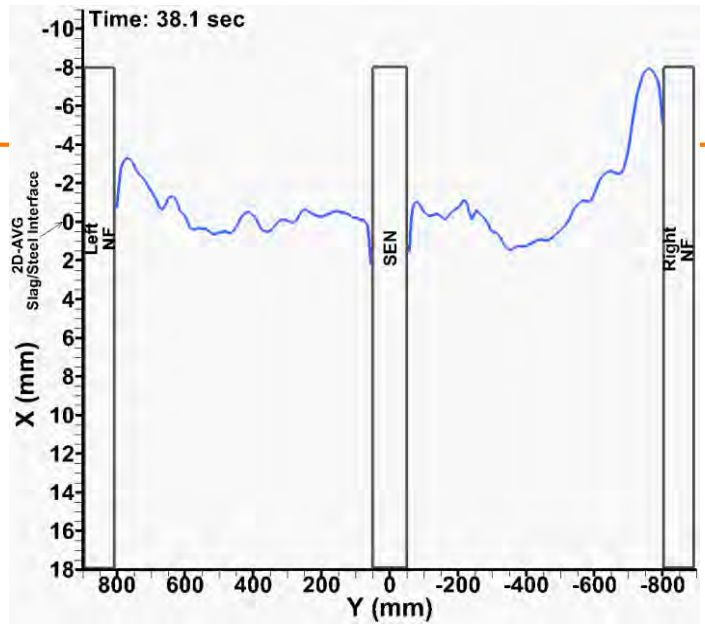

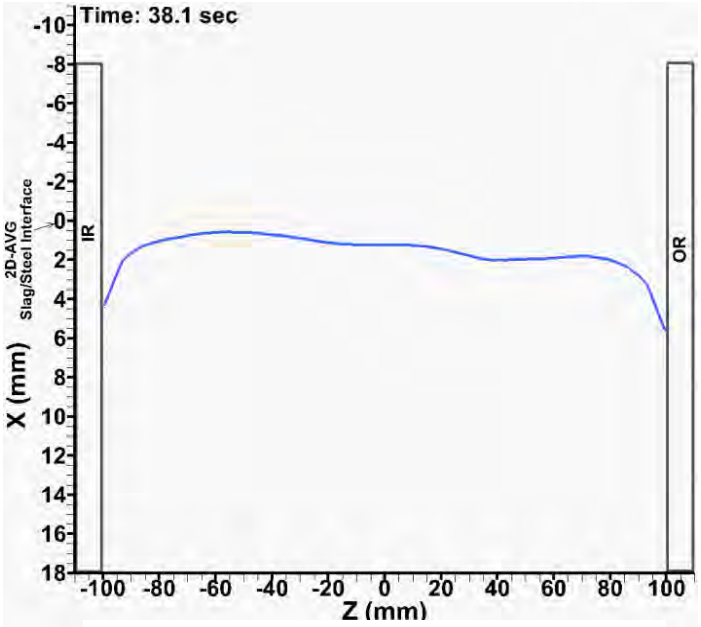

Case 2. -30° (down) angle

Effect of SEN Depth on Mold Flow Patterns

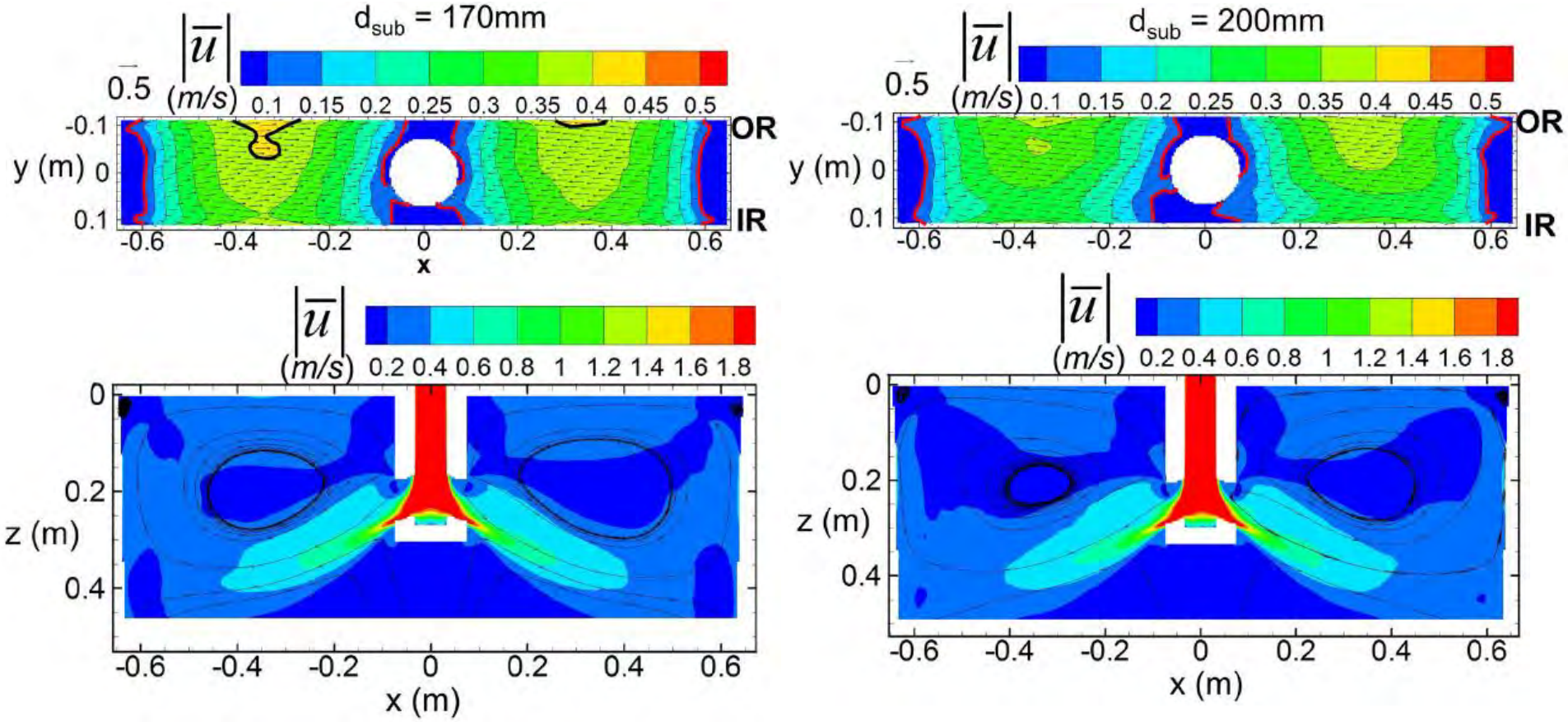

- Increasing submergence depth decreases top-surface velocity in mold: slag entrainment caused by instability at slag/molten steel interface, could be reduced

Double Ruler
ElectroMagnetic Braking (EMBr)

<Schematic of
Double ruler EMBr >

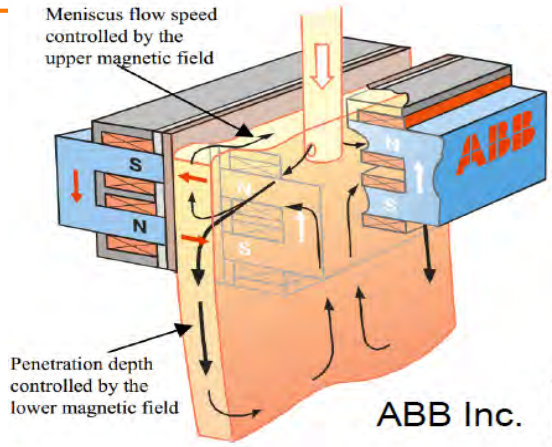

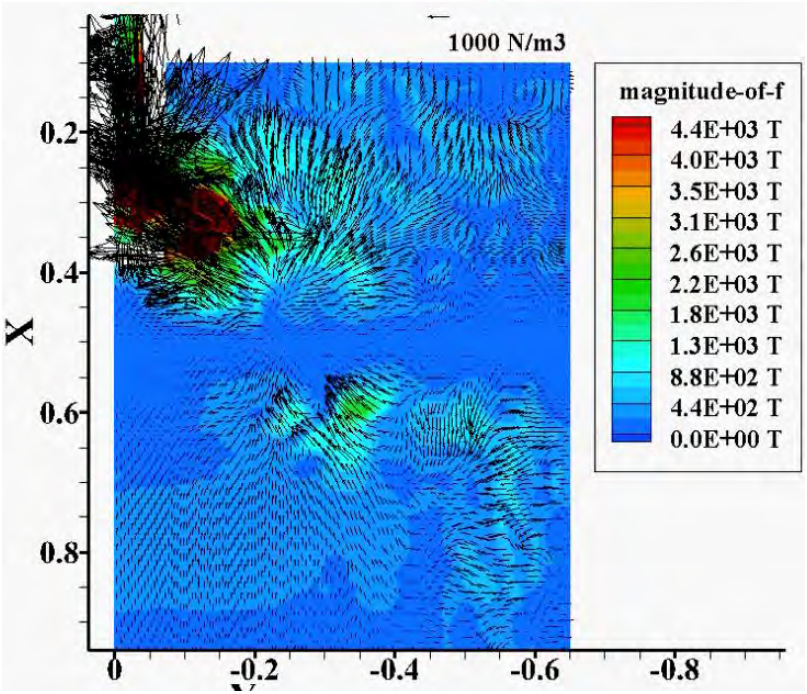

<Electromagnetic force on transient flow in CC>

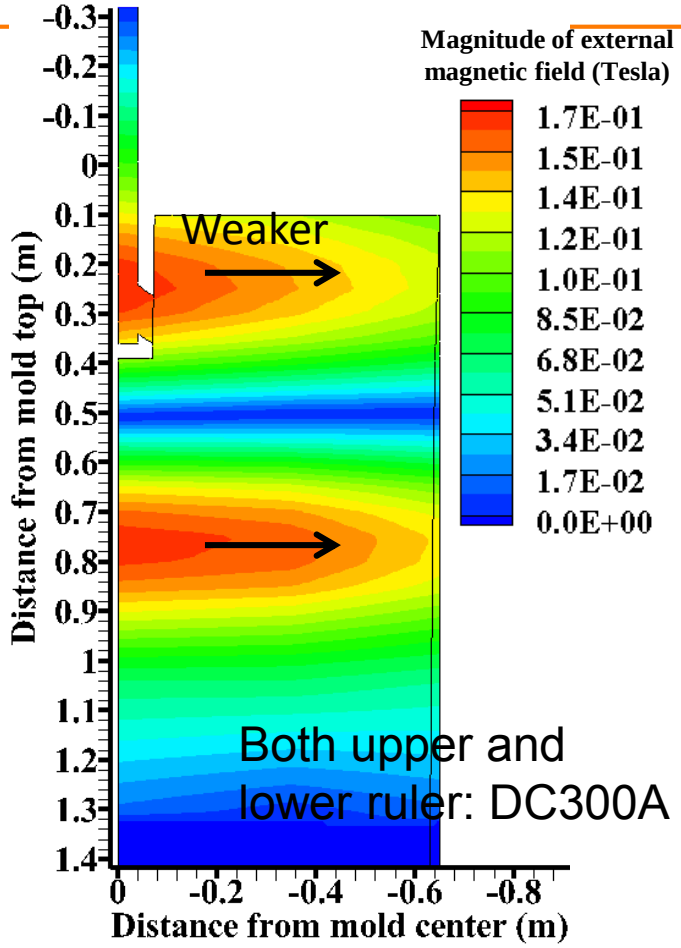

<External magnetic field by
Double ruler EMBr>

Effect of Double Ruler EMBr on Bubble Transport and Capture in Mold

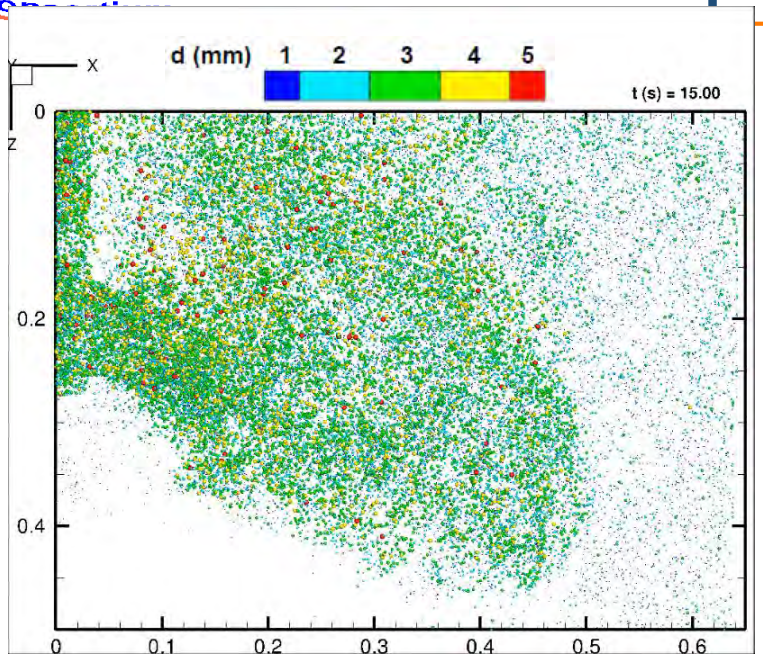

<Without EMBR>

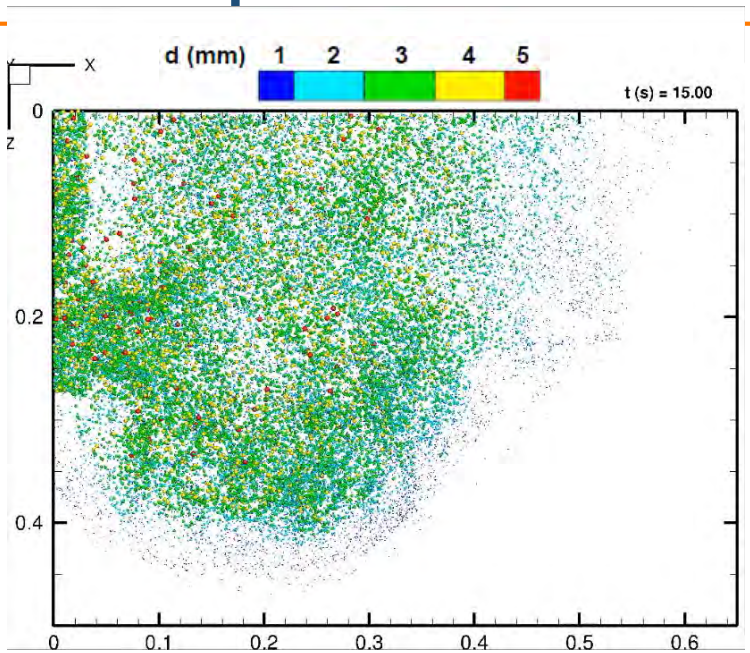

<With EMBR>

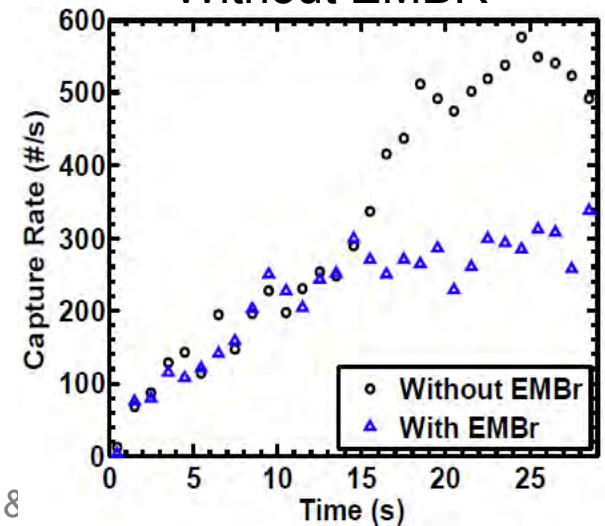

- With **EMBr**,
  Less bubbles reaching **NF**
  Less bubbles going deep into mold
- **EMBr reduces argon bubble capture** into steel shell; **less surface and internal defects**

* K. Jin: CCC 2016 annual report

Transient Mold Flow & Superheat Transfer on Solidifying Steel Shell in Mold

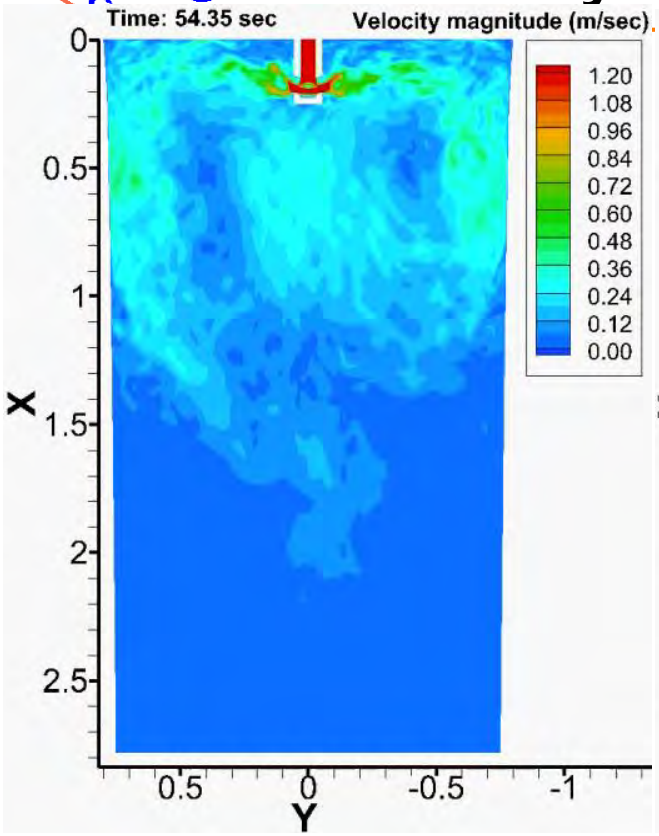

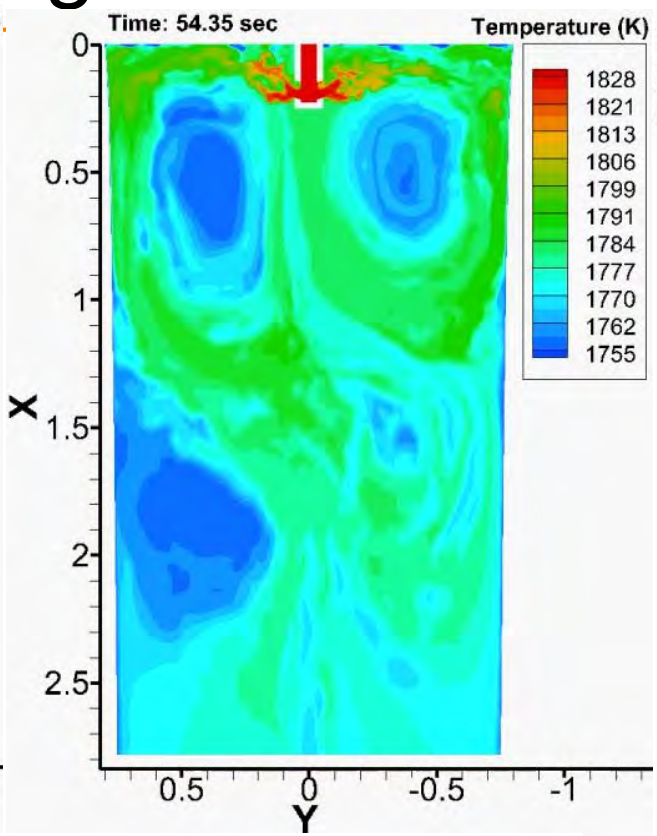

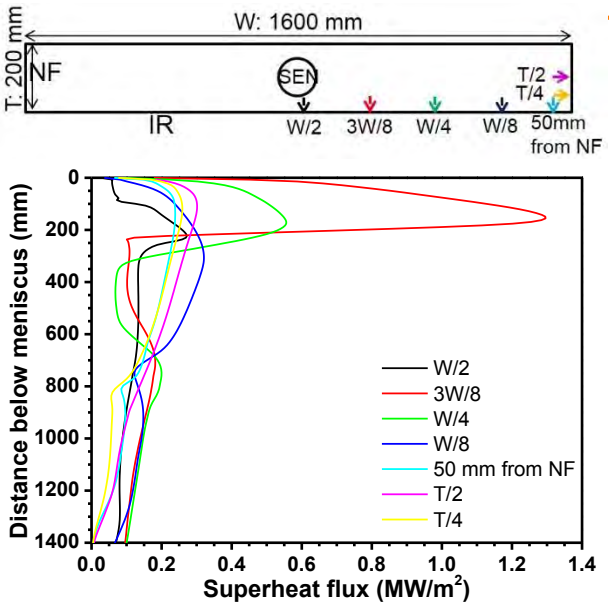

<Superheat flux on steel shell>

- **Temperature distribution** in mold shows transient behaviors according to **transient flow patterns**
- Due to **spread jet flow pattern in mold with +15° (up) angled nozzle port**, **superheat flux distribution** is **bigger on WF** than NF shells
- **Meniscus freezing** and **hook formation** on **corner** regions

<Hook defect and bubble capture>

Summary

- **Blue Waters supercomputing** has been applied to quantify **complex multiphysics phenomena** related to **defect formation** in **Continuous Casting (CC)** in order to **improve the process**
  - **Turbulent multiphase flow**: liquid mold flux/molten steel interface, molten steel-argon bubble flow
  - **Particle transport and capture**: argon bubble motion and capture into steel shell
  - **MagnetoHydroDynamics (MHD):** EMBr effect on flow pattern and argon bubble behaviors
  - Evaluation of **nozzle port angle**, **nozzle submergence depth**, and **EMBr strength**
- **Blue Waters resources (ANSYS Fluent HPC on BW XE nodes** and **In-house multi-GPU code**, **CUFLOW on BW XK nodes)** show **modeling capability breakthrough** (over 3000x faster) for **high-resolution** (less than 1mm length scale) **and huge-domain** simulation for CC**.**

Appendix I: Liquid Mold Flux/Molten Steel Interface Model: VOF

- **Volume fraction of each phase:**

$$\frac{\partial \alpha_{slag}}{\partial t} + \nabla \cdot \left(\alpha_{slag} \cdot \overrightarrow{u_{slag}}\right) = 0$$

slag volume fraction

$$\alpha_{steel} = 1 - \alpha_{slag}$$

steel volume fraction

- **Continuity:**

$$\frac{\partial \rho_{mix}}{\partial t} + \nabla \cdot \left(\rho_{mix} \vec{u}\right) = S_{shell,mass}$$

$$\rho_{mix} = \alpha_{steel}\rho_{steel} + \alpha_{slag}\rho_{slag}$$

$$S_{shell,mass} = -\frac{\rho_{steel} u_{casting} A}{V}$$

A: Projection of surface area of steel shell in casting direction

V: Volume of each cell with sink term

User Defined Function (UDF)

mass sink term to account for solidification of molten steel[*]

- **Momentum conservation:**

$$\rho_{mix}\frac{\partial u}{\partial t} + \rho_{mix} u \cdot \nabla u = -\nabla p + \nabla \cdot \left[\mu_{mix}\left(\nabla u + \nabla^T u\right)\right] + \rho_{mix} g + F_{interface} + S_{shell,mom}$$

$$F_{interface} = \sigma_{slag\text{-}steel} \frac{\rho_{mix}\kappa_{slag}\nabla\alpha_{slag}}{\frac{1}{2}\left(\rho_{steel} + \rho_{slag}\right)}$$

$$\kappa_{slag} = \nabla \cdot \hat{n} \qquad n = \nabla \alpha_{slag}$$

$$S_{shell,\,mom,i} = -\frac{\rho_{steel} u_{casting} A}{V} \bar{u}_i$$

UDF

momentum sink term in each component direction to consider solidification of molten steel[*]

* Yuan, Q., B. G. Thomas, and S. P. Vanka: MMTB, Vol. 35B:4, 2004, pp. 685-702

Appendix II: Bubble Transport Model

- **Two-way coupled Lagrangian particle tracking model**

F_D: Drag force
F_B: Buoyancy/gravity force
F_L: Lift force
F_A: Added mass force
F_P: Pressure gradient force

$$m_{Ar}\frac{du_{Ar}}{dt} = F_D + F_B + F_L + F_A + F_P$$

$$F_D = \frac{3}{4}\frac{C_D\mu}{(d_{Ar})^2}V_{Ar}(u - u_{Ar})Re_{Ar}$$

$$F_B = gV_{Ar}(\rho_{Ar} - \rho)$$

$$F_L = C_L\rho V_{Ar}(u_{Ar} - u)\times(\nabla\times u_{Ar})$$

$$F_A = \frac{1}{2}C_V\rho V_{Ar}\left(\frac{Du}{Dt} - \frac{du_{Ar}}{dt}\right)$$

$$F_P = \rho V_{Ar}\frac{Du}{Dt}$$

Drag coefficient[*]

$$C_D = \frac{16}{Re_{Ar}} \quad (Re_{Ar} < 0.49)$$

$$= \frac{20.68}{Re_{Ar}^{0.643}} \quad (0.49 < Re_{Ar} < 100)$$

$$= \frac{6.3}{Re_{Ar}^{0.385}} \quad (100 < Re_{Ar})$$

$$= \frac{We}{3} \quad \left(\frac{2065.1}{We^{2.6}} < Re_{Ar}\right)$$

$$= \frac{8}{3} \quad (8 < We)$$

$$Re_{Ar} = \frac{\rho d_{Ar}|u - u_{Ar}|}{\mu}$$

$$We = \frac{\rho d_{Ar}|u - u_{Ar}|^2}{\sigma_{steel-argon}}$$

$$S_{Ar} = -V_{cell}^{-1}\sum_{i=1}^{n}(F_D + F_B + F_L + F_A + F_P)$$

*J. T. Kuo and G. B. Wallis: Int. J. Multiphase Flow, Vol. 14 (1988), 547

Appendix III: Advanced Particle-Capture Model for Bubble Entrapment

Advanced particle capture criterion[1,2] when particle touches steel shell

- If particle diameter is smaller than primary dendrite arm spacing -> capture
- Else, compute 3 other forces: lubrication force, Van der Waals force, and interfacial concentration gradient force, and do force balance on particle to decide its capture

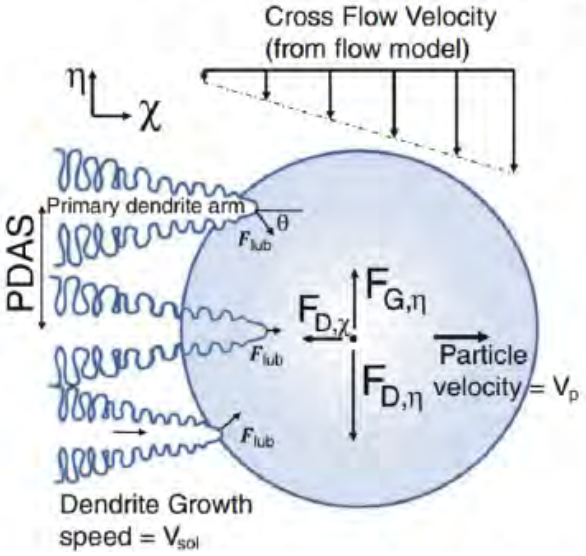

<Particle touching 3 dendrite tips [1]>

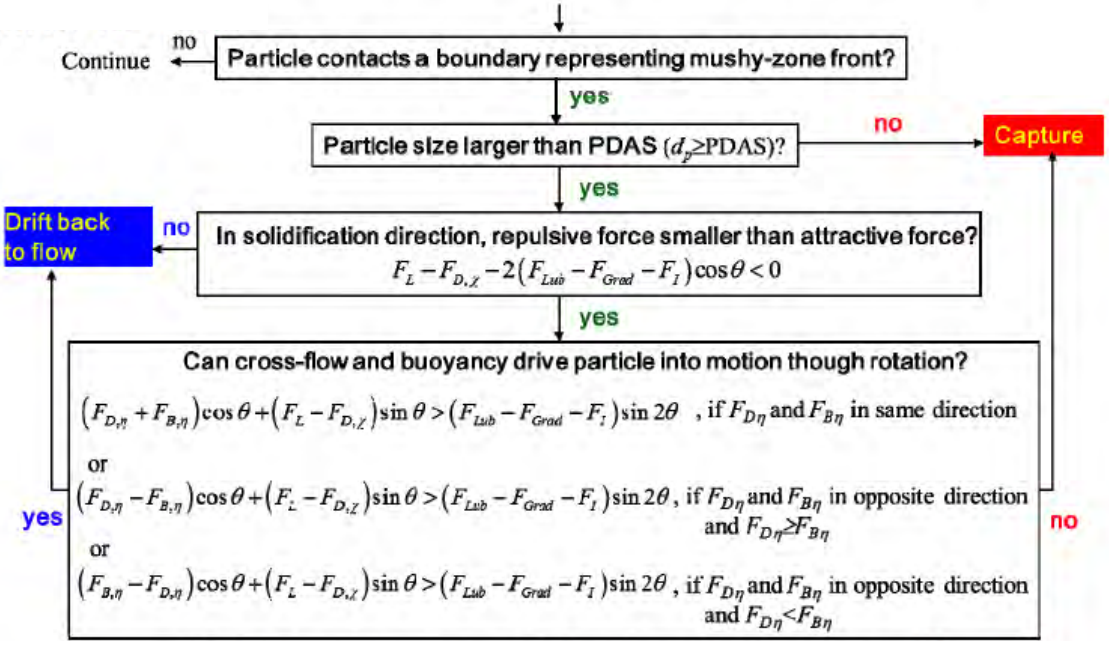

F_D: Drag force, F_B: Buoyancy force, F_L: Lift force, F_{Lub}: lubrication force, F_{Grad}: interfacial concentration gradient force, F_I: Van der Waals force

<Particle capture criterion flow chart [2]>

1. Q. Yuan: Ph.D. Thesis, UIUC, 2004
2. B. G. Thomas, Q. Yuan, S. Mahmood, R. Liu, and R. Chaudhary: MMTB, 2004, Vol. 45, pp. 22-35

Appendix IV: Nail Dipping Test

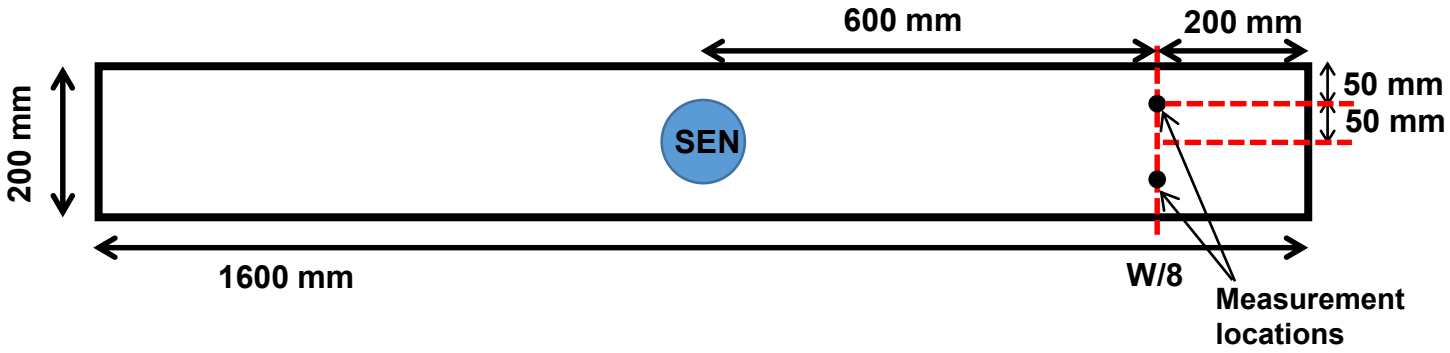

<Measurement locations in mold>

<Solidified lump from nail dipping test>

Dipping test details

Total tests (for each IR and OR region)	5
interval of each test	1 minute
Dipping time	3 sec

Empirical equation for surface velocity magnitude[*]:

$$\text{Surface velocity magnitude: } \mathbf{u_s\,(m/s)} = \mathbf{0.624} \cdot \left(\boldsymbol{\varphi}_{\mathbf{lump}}\,\mathbf{(mm)}\right)^{-0.696} \cdot \left(\mathbf{h_{lump}\,(mm)}\right)^{0.567}$$

* Liu et al., Proc. of TMS 2011,TMS, Warrendale, PA, USA